ELECTRICAL RESISTIVITY INVESTIGATION OF SOLID WASTE DISPOSAL SITE AT MAINTUMBI, MINNA, NIGER STATE

[1*]Arikewuyo, A., [2]Muhammad, A. and [3] Suleiman, I. K.
[1]*Department of Physics, Federal University of Technology, Minna*
[2,3]*Department of Physics, Ibrahim Badamasi Babangida University, Lapai*
*Corresponding author email: abdulbnarikewuyo@gmail.com

ABSTRACT

Electrical resistivity survey was conducted at an old waste dumpsite in Maitunbi, Chanchaga Local Government Area of Niger State in Nigeria to determine leachate contamination to soils, and its possible contamination to subsurface groundwater. The study area is mostly characterised by three (3) layered geologic sections which includes topsoil, weathered basement and Fresh basement. Thirty-Six vertical electric sounding (VES) lines were measured in a grid format on six profiles with spacing of about 20m intervals. The equipment used was the Abem Terrameter "SAS 4000", the data was analysed using computer processed methods with the following software; Winresist version 1.0 software, Surfer 10 software programmes. The analysis indicates that there was an ingress of leachate contaminant at the dumpsite with a very low resistivity of 20 Ωm to 60 Ωm as compared to that of control site of resistivities 200 Ωm to 850. The result shows that the leachate was localized at about 13m from the topsoil of the dumpsite and is spreading in the direction of the groundwater flow. However, considering the weathered/fractured layer thickness map, the aquifer is observed to be promising at the depth of 20 m. This suggests that the ground water is not contaminated. But if the migration continues at the current rate of 1.63 m/year, the ground water will be contaminated in 12.3 years from now if proper mitigation measures are not taken into consideration at the dumpsite.

Keywords: Leachate, Terrameter, Groundwater, Zoody software, Contamination, Aquifer.

INTRODUCTION

Fast industrial development and the uncontrolled growth of the urban population results in the production of toxic solid wastes. Urban waste materials, mainly domestic garbage, are usually disposed of inadequately in waste disposal sites posing a high risk to the underground water resources, the environmental pollution, and the community health. The solution to the day-to-day problems of modern urban societies demands fast and effective geophysical methods.

Groundwater pollution is caused by the presence of undesirable and hazardous material and pathogens beyond certain limits. Much of the pollution is due to anthropogenic activities like discharge of sewage, effluents and waste from domestic and industrial establishment. Also, the situation of groundwater pollution is more pronounced during the rainy season owing to the rate of leachate infiltration, percolation and migration.

The importance of groundwater as a valuable source of portable water cannot be overemphasised. Groundwater forms part of the most important natural resources of any region and compliment surface sources in the provision of portable water for domestic and industrial application. The populace is also dependent on the abundance, fertility and integrity of the soils for agriculture, shelter, and other economic and industrial activities (Jatau and Ajodo, 2016).

Unfortunately, the quality of these natural resources has been impaired by the indiscriminate location of dumpsites without regards to health of the people and damage to the environment.

Geoelectrical method has been found very suitable for this kind of environmental study. This is due to the fact that generally, ionic concentration of leachate is much higher than that of groundwater and so when the leachate enters the aquifer, it results in a large contrast in electrical properties and the method will identify these zones as an anomaly which enables the leachate plume to be detected (Asurimen, 2008).

STATEMENT OF THE PROBLEM

The study area is surrounded by a good number of plots of land demarcated by beacons which suggests the possibility of its use for residential purposes as a result of population growth and rapid expansion of Minna town. An example of such site is the plot belonging to Nigeria Union of Teachers (NUT) which is just about 50 m from the refuse disposal site.

A research carried out by Aderoju*et.al* (2014)., on a Geo-Spatial Approach for Solid Waste Dumpsites for Sustainable Development in Minna, Niger State, Nigeria discovers that the identified built-up areas within a distance of 1000m to dumpsites location showed that BossoEstate, Mypa, Dutsen Kura, Western bypass, Maitumbi, Tunga, Chanchanga, Shango, Kpakungu, Sokakahuta are at risk of possible environmental problems.

The health risks, if leachate is left untreated and allowed to contaminate groundwater supplies include skin irritation (Plate II), nausea, vomiting, and headache, while chronic exposure can lead to anemia, kidney damage, prostate cancer, lung cancer, memory loss, coma, headaches and depression (Manoj *et. al*., 2014). Therefore, it has become imperative to study the area and make recommendation to relevant authorities regarding the impeding health risk associated with contaminated underground water to the citizens. The sitting of boreholes as the source of potable water in this area will be a very serious challenge. The challenge is worsened by the fact that there are inadequately trained waste disposal personnel.

Location and Accessibility of the Study Area

The study area Maitumbi disposal site is located between latitudes 09 40'37.17 to 09 41'37.15 N (Figure 1.1) and longitudes 06 29'51.66'' to 06 30'51.55 E. The area lies within the south western part of Minna metropolis and is accessible through Minna-Sarkin Power road. The area has a typical Guinea savannah climate with distinct wet and dry seasons: A dry season which usually last from December to March and an accompanied rainy season which last from April to October. Relative humidity at sunrise during raining season is about 75% and very low during dry season.

Geology and Hydrogeology of the Study Area

Minna occupies the central portion of the Nigerian basement complex which lies on a batholith (Udensi *et al.*, 1986). The Minna area falls within the larger northwestern Nigerian Basement Complex. The rocks of the area are mostly crystalline rocks consisting of Gneisses and Migmatites, and Meta-Sedimentary Schist (Mohammed *et. al*, 2008). The area is thus underplayed by two lithological units of Granites and Gneisses rocks with Pegmatite's and quartz veins as minor intrusive. The Granites rocks, which cover about 80% of the area, are mostly exposed on the western part of the town. They mostly form high batholiths, which are extensive in size. The Granitic outcrops are highly jointed, fractured, foliated and in some places appear as boulders (Adeniyi, 1985). The second lithological unit, the Gneiss, covers about 20% of the area and occurs to the east of city. They are fine grained with gneissose banding defined by the alternating lighter coloured minerals (quartz and feldspars) and the dark coloured ones (biotite micas).

Hydrogeophysically, Minna area is made up of only crystalline hydrogeological province, as there is a complete absence of sedimentary rocks in the study area. This crystalline hydrogeological province is made up of two interconnected aquifers, namely:

i. the aquifer within the overburden/weak zone and
ii. the partial Weathered/Fractured Basement aquifer.

Figure 1: Map showing the geology of Niger State

METHODOLOGY

The procedure employed in this research is as follows:

i. Profiling
ii. data collection
iii. data analysis
iv. interpretations

ABEM SAS 4000 model was used for the data collection on the field. Both current and voltage reading s were collected and later converted to resistance values with the help of Ohm's law($R = V/I$). The resistance value was multiplied by the geometric factor (k-factor) gives the resistivity.

VES points A1 to A6 represents profile A and VES points F1 to F6 represents profile F, respectively. In order to locate these VES points after the field survey, GPS was used to collect the coordinates and topography readings for each VES point.

ABEM terrameter was finally set up by inserting both the current and potential electrode into the ground while ensuring tight connections of the terminals.

DATA COLLECTION

The area under review was inspected, measured and gridded into six profiles; A-F (Figure 2a). The length of each profile is 100 m, the distance between one profile and the other is 20m. The control site which is about100m away from the dump site and separated by anexpress road from the study area was also gridded into profiles A′-C′ (Figure 2b). The length of each control profile is 40 m and the inter profile spacing is 20 m.

Vertical electrical sounding was carried out on thirty-six (36) points marked with pegs using Schlumberger spread of electrode configuration on the dumpsite which is the study area, while another nine (9) VES points was carried out using the same Schlumberger spread of electrode on the control area.

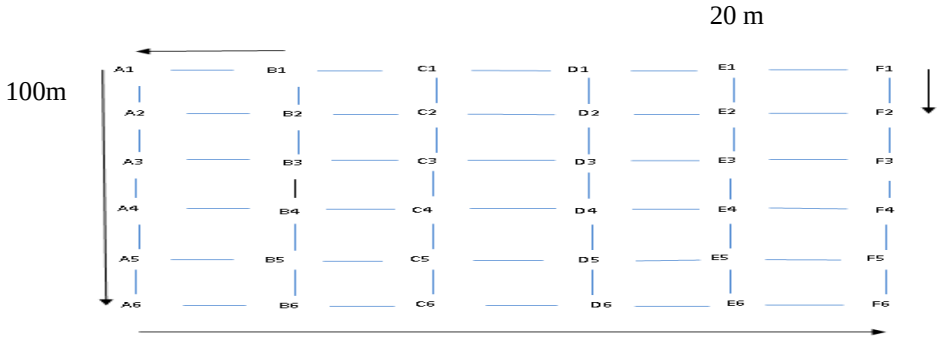

Figure 2a: Profile layout and location of the VES points on dump site

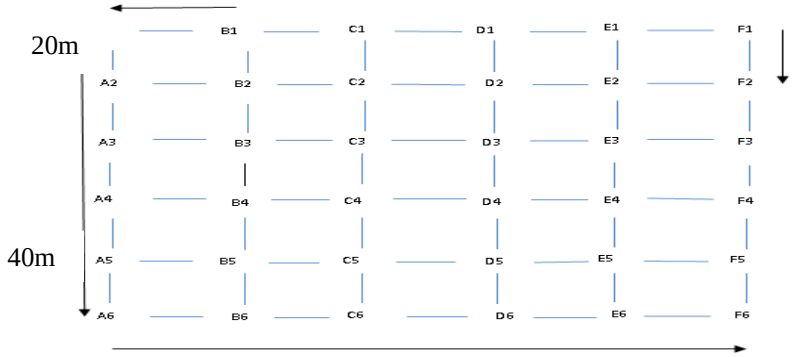

Figure 2b: Profile layout and location of the VES points on control site

The estimated resistance value on the terrameter was later multiplied by the geometric factor, K to obtain the apparent resistivity. The apparent resistivity data obtained from the VES survey was presented as depth sounding curves by plotting the apparent resistivity along the ordinate axis and the half current electrode spacing (AB/2) along the abscissa. The resistivity curves were classified based on layer resistivity, the number of layers in the subsurface and the thickness of each layer.

Potential in Homogeneous Media

Current flows radially away from the source and the potential varies inversely with distance from the current source. The equipotential surfaces have a hemisphere

shape, and the current flow is perpendicular to the equipotential surface. The potential in this case is given by:

$$\phi = \frac{\rho l}{2\pi r} \qquad (1)$$

where r is the distance of a point in the medium (including the ground surface) from the electrode. In practice, all resistivity surveys use at least two current electrodes, a positive current and a negative current source. The potential values have a symmetrical pattern about the vertical place at the mid-point between the two electrodes. The potential value in the medium from such a pair is given by:

$$\phi = \frac{\rho l}{2\pi r}\left(\frac{1}{r_{C1}} - \frac{1}{r_{C2}}\right) \qquad (2)$$

where $r_{C1}$and r_{C2} are distances of the point from the first and second current electrodes. In principle, the potential difference between two points (normally on the ground surface) is measured.

$$\Delta\phi = \frac{\rho l}{2\pi}\left(\frac{1}{r_{C1p1}} - \frac{1}{r_{C2p1}} - \frac{1}{r_{C1p2}}\frac{1}{r_{C2p2}}\right) \qquad (3)$$

The above equation gives the potential that would be measured over a homogenous medium with four (4) electrodes array.

Actual field surveys are invariably conducted over an inhomogenous medium where the subsurface resistivity has a 3-D distribution. The resistivity measurements are still made by injecting current into the ground through the two current electrodes (C1 and C2) and measuring the resulting voltage difference at two potential electrodes (P1 and P2).From the current (I) and potential($\Delta\phi$) values, apparent resistivity (ρ_a) value is calculated.

$$\rho_a = \frac{k\Delta\phi}{I} \qquad (4)$$

where k is the geometric factor given by

$$k = \frac{2\pi}{\frac{1}{r_{C1p1}} - \frac{1}{r_{C2p1}} - \frac{1}{r_{C1p2}}\frac{1}{r_{C2p2}}} \qquad (5)$$

ρ_a is the resistivity of the material and
I is the current.

Data Analysis and Interpretations

The VES interpretation was carried out using computer software called WinRESIST version 1.0. The plotted curves obtained give the equivalent n-layered model from the apparent resistivity of each sounding point. Surfer 10 computer software was used to produce iso-resistivity and geoelectric vertical section contour maps of data deduced from the WinRESIST curves. This gives more lithology information about the study area.

Summary of the Vertical Electrical Sounding (VES) Analysis along the Profiles

The resistivity – depth curves were plotted using WinResist version 1.0 software package for automatic interpretation of Schlumberger sounding as shown in appendix A. The number of layers, depth, thickness and average resistivity for each VES points were also determined from the plotted curves which were eventually summarised in tabular form for both dumpsite and control site as shown in Tables 1-5, respectively. Vertical geo-electric section maps, fracture basement thickness map, basement and Iso-resistivity maps were also produced to determine the migration of leachates in the subsurface.

Table 1 shows the summary of the resistivity result for profile A. the whole profile shows three layers model. The profile shows two distinct curve types including H (VES A1, A2, A3 and A4) and A (VES A5 and A6). The first layer has a resistivity value ranging from 18.6 Ωm to 349.3 Ωm. The lowest resistivity value of 18.6 Ωm is found at VES A5 while the highest resistivity value of 349.3Ωm is found at VES A2. The layer has the highest thickness of 20.0m at VES A5 while the lowest thickness of 0.5m is located at VES A1. The second layer has resistivity value ranging between69.82 Ωm to 413.5 Ωm. the lowest resistivity value of 69.82Ωm is located at VES A3 while the point with the highest resistivity value of 413.5 Ωm is at VES A6. The layer has thickness ranging from 3.0 m at VES A6 to 50m at VES A5. The third layer has characterized by resistivity value ranging from 802.65 Ωm to 1748.7 Ωm. the lowest resistivity value of 802.65 Ωm located at VES A2 while the highest of 1748.7 Ωm at VES A5. The layer's thickness is to infinity depth.

The summary of the resistivity result for profile B is shown in table 1. The whole profile shows three layers model except VES B1 and B6 that are characterized by two layers model. The profile shows three distinct curve types including A (VES B1, B5 and B6), H (VES B2) and K (VES B3 and B4). The first layer has a resistivity value ranging from 0.6 Ωm to 42.2 Ωm. the lowest resistivity value of 0.6 Ωm is found at VES B1 while the highest resistivity value of 42.2 Ωm is found at VES B5. The layer has the highest thickness of 30.0m at VES B4 while the lowest thickness of 0.3m located at VES B1. The second layer is typified by resistivity ranging from 7.35 Ωm to 1925 Ωm. The lowest resistivity of 7.35 Ωm is located at VES B2 and the highest which is located at VES B6 is 1925 Ωm. the layer has the highest thickness of 47.0m at VES B3 and the lowest thickness of 2.6 at

VES B5. As for the Third layer, the resistivity ranges from 112.2 Ωm to 873.7 Ωm. the lowest resistivity of 112.2 Ωm is located at VES B3 and the highest of 873.7 Ωm is located at VES B5. The layer's thickness is to infinity depth.

The summary of the resistivity result for profile C is shown in table 2. The whole profile shows three layers model except VES C1 and C6 that are characterized by two layers model. The profile shows a singular curve type of type A.The first layer has a range of resistivity value from 0.9 Ωm to 248.8 Ωm. the layer's resistivity is lowest at VES C4 which is 0.9 Ωm and highest at VES C1 which is 248.8 Ωm. the layer has the highest thickness of 15.0m at VES C6 and lowest thickness of 0.3m at VES C4. The second layer is characterized by resistivity values ranging from 27.23 Ωm to 2446.6 Ωm. the layer's resistivity is lowest at VES C5 with 27.23 Ωm while it is highest at VES C1 with 2446.6 Ωm. The layer has the highest thickness of 54.0 at VES C5 and the lowest thickness of 4.1m at VES C4. The third layer has a range of resistivity value from 112.0 Ωm to 23619.5 Ωm. The layer has the lowest resistivity of 112.0 Ωm at VES C3 and the highest value of 23619.5 Ωm at VES C4. The layer's thickness is to infinity depth.

The summary of the resistivity result for profile D is shown in table 2. The whole profile shows three layers model except VES D4 that is characterized by two layers model. The profile shows a singular curve type of type A. The first layer has a resistivity value ranging from 1.2 Ωm at VES D2 to 85.6 Ωm at VES D6. The layer has lowest thickness of 0.8 m at D2 and D6 and highest thickness of 20.0 m at VES D4. The second layer has the lowest resistivity value of 43.7 Ωm at VES D1 and the highest value of 18693.8 at VES D4. The layer's thickness is lowest at VES D2 and D3 with 3.4m and highest at VES D6 at 38.0m. The third layer has a resistivity value ranging from 414.7 Ωm at VES D3 to 31832.9 Ωm at VES D6. The layer's thickness is to infinity.

The summary of the resistivity result for profile E is shown in table 3. The whole profile shows Three layers model except VES E5 that is characterized by Two layers model. The profile shows two distinct curve types including A (VES E3, E4 and E5) and H (VES E1, E2 and E6). Layer one is characterized by resistivity value ranging from 0.6 Ωm at VES E4 to 19.5 Ωm at VES E1. The layer has the lowest thickness of 2.0m at VES E6 while the highest thickness of 30.0m is at VES E2. Layer two has resistivity value ranging from 0.2 Ωm at VES E6 to 233.9 at VES E5. The layer has the lowest thickness of the 3.0m at VES E1 and the highest thickness of 27.0m at VES E4. The third layer is characterized by resistivity value ranging from 48.35 Ωm at VES E6 to 529.4 Ωm at VES E3. The depth of the layer is to infinity.

Table 1: Summary of VES analysis along profile A and B (Dump site)

VES Points	Curve Type	No of Layers	Depth (m)	Thickness (m)	Resistivity (Ωm)	VES Points	Curve Type	No of Layers	Depth (m)	Thickness (m)	Resistivity (Ωm)
	H	1	0.0	0.5	230.4	B1	A	1	0.0	0.3	0.6
		2	0.5	20.0	150.13			2	0.3	∞	463.1
A1		3	20.5	∞	1242.5	B2	H	1	0.0	3.0	16.2
A2	H	1	0.0	1.9	349.3			2	3.0	12.0	7.35
		2	1.9	4.9	75.2			3	15.0	∞	181.8
		3	6.8	∞	802.65	B3	K	1	0.0	3.0	2.9
A3	H	1	0.0	1.3	283.75			2	3.0	47.0	284.6
		2	1.3	8.3	69.82			3	50.0	∞	112.2
		3	9.6	∞	1231.24	B4	K	1	0.0	30.0	9.6
A4	H	1	0.0	0.8	227.0			2	30.0	30.0	145.4
		2	0.8	8.9	100.83			3	60.0	∞	660.0
		3	9.7	∞	1653.65	B5	A	1	0.0	5.0	42.2
A5	A	1	0.0	20.0	18.6			2	5.0	2.6	318.8
		2	20.0	50.0	409.4			3	7.6	∞	873.7
		3	70.0	∞	1748.7	B6	A	1	0.0	2.6	12.6
A6	A	1	0.0	4.9	39.95			2	2.6	∞	1925.0
		2	4.9	3.0	413.5						
		3	7.9	∞	927.6						

Table 2: Summary of VES analysis along profile C and D (Dump site)

VES Points	Curve Type	No of Layers	Depth (m)	Thickness (m)	Resistivity (Ωm)	VES Points	Curve Type	No of Layers	Depth (m)	Thickness (m)	Resistivity (Ωm)
	H	1	0.0	0.5	230.4	B1	A	1	0.0	0.3	0.6
		2	0.5	20.0	150.13			2	0.3	∞	463.1
A1		3	20.5	∞	1242.5	B2	H	1	0.0	3.0	16.2
A2	H	1	0.0	1.9	349.3			2	3.0	12.0	7.35
		2	1.9	4.9	75.2			3	15.0	∞	181.8
		3	6.8	∞	802.65	B3	K	1	0.0	3.0	2.9
A3	H	1	0.0	1.3	283.75			2	3.0	47.0	284.6
		2	1.3	8.3	69.82			3	50.0	∞	112.2
		3	9.6	∞	1231.24	B4	K	1	0.0	30.0	9.6
A4	H	1	0.0	0.8	227.0			2	30.0	30.0	145.4
		2	0.8	8.9	100.83			3	60.0	∞	660.0
		3	9.7	∞	1653.65	B5	A	1	0.0	5.0	42.2
A5	A	1	0.0	20.0	18.6			2	5.0	2.6	318.8
		2	20.0	50.0	409.4			3	7.6	∞	873.7
		3	70.0	∞	1748.7	B6	A	1	0.0	2.6	12.6
A6	A	1	0.0	4.9	39.95			2	2.6	∞	1925.0
		2	4.9	3.0	413.5						
		3	7.9	∞	927.6						

Table 3: Summary of VES analysis along profile E and F (Dump site)

VES Points	Curve Type	No of Layers	Depth (m)	Thickness (m)	Resistivity (Ωm)	VES Points	Curve Type	No of Layers	Depth (m)	Thickness (m)	Resistivity (Ωm)
E1	A	1	0.0	3.0	0.3	F1	A	1	0.0	3.0	0.3
		2	3.0	67.0	36.8			2	3.0	67.0	36.8
		3	70.0	∞	60.4			3	70.0	∞	60.4
E2	A	1	0.0	5.6	8.9	F2	A	1	0.0	5.6	8.9
		2	5.6	27.3	429.93			2	5.6	27.3	429.93
		3	32.9	∞	3391.1			3	32.9	∞	3391.1
E3	A	1	0.0	1.9	0.4	F3	A	1	0.0	1.9	0.4
		2	1.9	1.9	0.7			2	1.9	1.9	0.7
		3	3.8	∞	124.7			3	3.8	∞	124.7
E4	A	1	0.0	10.0	7.9	F4	A	1	0.0	10.0	7.9
		2	10.0	20.0	125.9			2	10.0	20.0	125.9
		3	30.0	∞	1196.1			3	30.0	∞	1196.1
E5	A	1	0.0	1.3	0.8	F5	A		0.0	1.3	0.8
		2	1.3	∞	711.2			2	1.3	∞	711.2
E6	A	1	0.0	3.0	0.1	F6	A	1	0.0	3.0	0.1
		2	3.0	12.0	16.7			2	3.0	12.0	16.7
		3	15.0	∞	436.6			3	15.0	∞	436.6

Table 4: Summary of VES analysis along profile A' and B' (Control site)

VES Points	Curve Type	No of Layers	Depth (m)	Thickness (m)	Resistivity (Ωm)	VES Points	Curve Type	No of Layers	Depth (m)	Thickness (m)	Resistivity (Ωm)
A 1	H	1	0.0	0.9	899.8	B'1	K	1	0.0	1.3	310.6
		2	0.9	1.6	45.4			2	1.3	45.3	354.1
		3	2.5	∞	841.0			3	46.6	∞	1386.1
A'2	H	1	0.0	0.6	907.5	B'2	H	1	0.0	0.8	595.8
		2	0.6	11.4	159.7			2	0.8	28.6	224.4
		3	12.0	∞	2893.7			3	29.4	∞	1044.2
A'3	H	1	0.7	0.7	892.4	B'3	H	1	0.0	0.9	344.6
		2	0.7	10.3	153.45			2	0.9	2.4	12.5
		3	11.0	∞	862.0			3	3.3	∞	823.9

Table 5: Summary of VES analysis along profile C' (Control site)

VES Points	Curve Type	No of Layers	Depth (m)	Thickness (m)	Resistivity (Ωm)
C'1	H	1	1.3	1.3	514.4
		2	5.7	4.4	46.4
		3	10.1	∞	1050.5
C'2	H	1	0.0	0.5	4475.5
		2	0.5	7.7	148.4
		3	8.2	∞	3792.9
C'3	H	1	0.0	2.8	382.3
					238.4
					20524.6

The summary of the resistivity result for profile F is shown in Table 3. The whole profile shows three layers model except VES F5 that is characterized by two layers model. The profile shows a singular curve type of type A. The resistivity of the first layer ranges from 0.1 Ωm at VES F6 to 8.9 Ωm at F2. The layer has the lowest thickness of 1.3 at F5 and the highest thickness of 10.0 m at VES F4. Layer two has resistivity value ranging from 0.7 Ωm at VES F3 to 711.2 Ωm at F5. The layer has the lowest thickness of 1.9m at F3 and the highest thickness of 67.0 m at VES F1. The third layer is characterized by resistivity value ranging from 60.4 Ωm at VES F1 to 3391.1 Ωm at F2. The layer's thickness is to infinity.

The summary of the VES analysis along profile A' is shown in table 4.The profile is underlain by 3 layers which are topsoil, fractured basement and fresh/ competent basement. The profile shows a singular curve type of type H. The resistivity of the first layer ranges from 892.4 Ωm at VES A'3 to 907.5 Ωm at A'2. The layer has the lowest thickness of 0.6m at A'2 and the highest thickness of 0.9m at VES A'1. Layer two has resistivity value ranging from 45.4 Ωm at VES A'1 to 159.7 Ωm at A'2. The layer has the lowest thickness of 1.6m at A'1 and the highest thickness of 11.4 m at VES A'2. The third layer is characterized by resistivity value ranging from 841.0 Ωm at VES A'1 to 2893.7 Ωm at A'2. The thickness is to infinity.

The summary of the VES analysis along profile B' is shown in Table 4.The profile is underlain by 3 layers which are topsoil, fractured basement and fresh/ competent basement. The profile shows curve type K at VES B'1 and H at VES B'2 and B'3. The resistivity of the first layer ranges from 310.6 Ωm at VES B'1 to 595.8 Ωm at B'2. The layer has the lowest thickness of 0.8m at B'2 and the highest thickness of 1.3m at VES B'1. Layer two has resistivity value ranging from 12.5 Ωm at VES B'3 to 354.1 Ωm at B'1. The layer has the lowest thickness of 2.4m at B'3 and the highest thickness of 45.3 m at VES B'1. The third layer is characterised by resistivity value ranging from 823.9 Ωm at VES B'3 to 1386.1 Ωm at B'1. The layer's thickness is to infinity.

The summary of the VES analysis along profile C' is shown in Table 5. The profile is underlain by 3 layers which are topsoil, fractured basement and fresh/ competent basement. The profile shows curve type H at all VES points. The resistivity of the first layer ranges from 382.3 Ωm at VES C'3 to 4475.5 Ωm at C'2. The layer has the lowest thickness of 0.5 m at C'2 and the highest thickness of 2.8 m at VES C'3. Layer two has resistivity value ranging from 46.4 Ωm at VES C'1 to 238.4 Ωm at C'3. The layer has the lowest thickness of 4.4 m at C'1 and the highest thickness of 10.3 m at VES C'3.The third layer is characterized by resistivity value ranging from 1050.5 Ωm at VES C'1 to 20524.6 Ωm at C'3. The layer's thickness is to infinity.

Sample of Iso-Resistivity Contour Maps at Various Depths

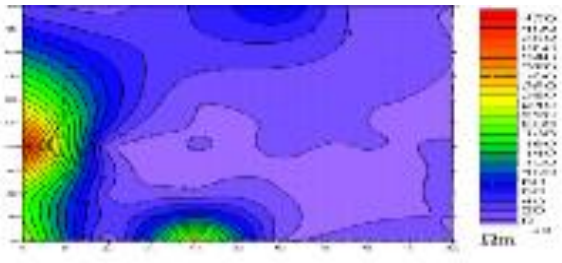

Figure 3a: Dump site iso-resistivity map at the surface

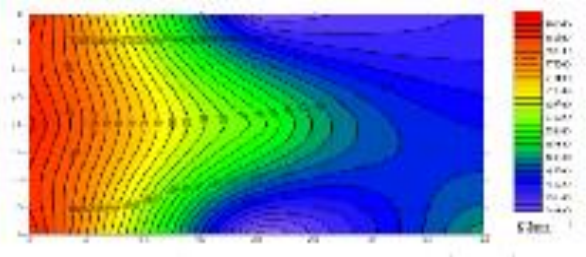

Figure 3b: Control site iso-resistivity map at the surface

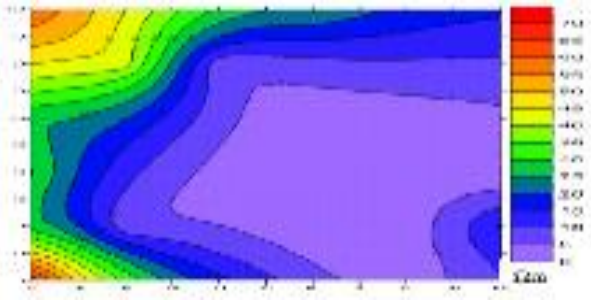

Figure 4a: Dump site iso-resistivity map at 5m

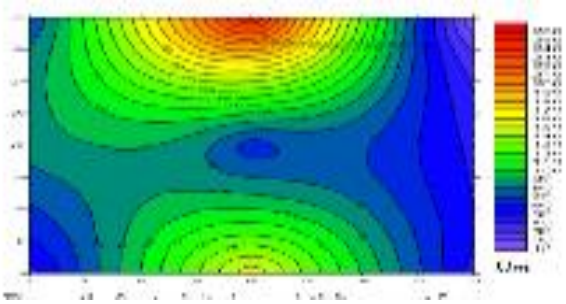

Figure 4b: Control site iso-resistivity map at 5m

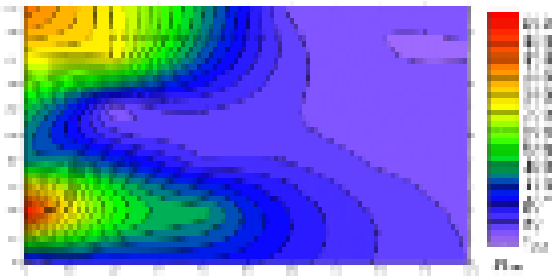

Figure 5a: Dump site iso-resistivity map at 10m

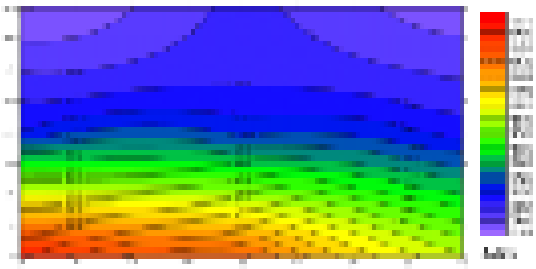

Figure 5b: Control site iso-resistivity map at 10m

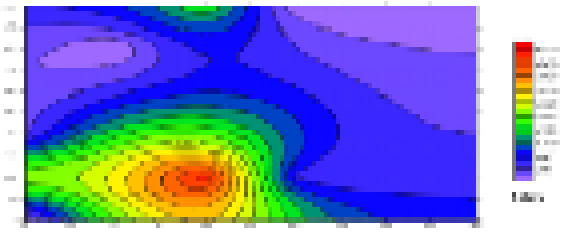

Figure 6a: Dump site iso-resistivity map at 20m

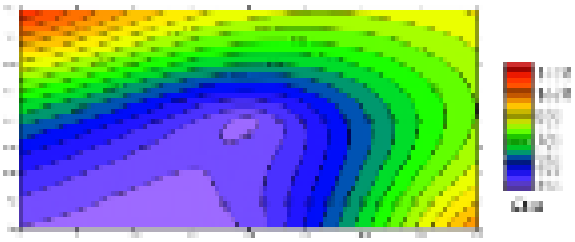

Figure 6b: Control site iso-resistivity map at 20m

Deduction and correlation of iso-resistivity maps at the surface

Figure 3a and 3b below shows the iso-resistivity maps of the dump and control sites respectively at the surface. The contour interval for the maps is 20 Ωm for the dump and control sites. The maps are produced in other to monitor the level of contamination at the surface which is done by comparing the two maps. The resistivity value at the dump site ranges from 20 Ωm to 220 Ωm with 20 Ωm to 40 Ωm covering a very large percentage of the total area. The area that lies along profile A is seen to have high resistivity which is an indication of absence of contaminant on that profile. Meanwhile, the resistivity value of the map on the control site ranges from 380 Ωm to 820 Ωm. The two maps compared shows the presence of leachate on the dump site. According to Abdullahi *et al*, the low apparent resistivity end <80 Ωm could be attributed to contamination of the groundwater due to leachate invasion (Abdullahi *et al*, 2010) This is in tandem with the summary of VES analysis presented in tabular form above.

Deduction and correlation of iso-resistivity maps at the depth of 5m

The same map was produced for the two sites at the depth of 5m. This is to determine the movement of the contaminant at the subsurface. Figure 4a and 4b shows the iso-resistivity maps of the dump and control sites respectively at the depth of 5m. The contour interval for the maps are 5 Ωm and 10 Ωm for dump and control sites respectively. The resistivity value at the dump site ranges from 5 Ωm to 45 Ωm which is low as compared to the control site at the same depth. The resistivity

value of the map on the control site on the other hand ranges from 60 Ωm to 200 Ωm. the two maps compared shows the presence of The vertical geo-electric section of profile A is as shown in figure (4.8a) while its corresponding geologic section is shown in figure (4.8b). The map is contoured at an interval of 70 Ωm. This map can be divided into three layers**.**

Interpretation of Iso-resistivity Contour Map at 10 m
The Iso-resistivity Map at 10 m depth is as shown in figure (5a and 5b). The map is contoured at interval of 30 Ωm. The resistivity varies from 60 Ωm to 960 Ωm across the field. The relatively high resistivity value observed at the south-western part of the study area is due to the lateritic/gravels content found on the site and this is immediately accompanied by a low resistivity region at the North-eastern part of the study area. This region has resistivity value ranging between 30 Ωm to 150 Ωm which could be attributed to the presence ground water (VES D3). The fractured or fairly weathered basement could be found prominently at south-western part of the map (i.e. VES B1) with resistivity value ranging between 240 Ωm and 460 Ωm.

Interpretation of Iso-resistivity Contour Map at 20 m
The Iso-resistivity Map at 20 m depth is as shown in figure (6a and 6b). This is very similar to map obtained at 15 m depth only that those areas that are said to be fractured now have the resistivity value of 1000 Ωm and above and this corresponds to the shaded part of figure The map is contoured at interval of 50 Ωm. The resistivity varies from 50 Ωm to 750 Ωm. It can be observed here that the weathered lateritic content found at the southern part of (figure 6a) also continued at the central part of (figure 6b) and South-Western part of the iso- resistivity map at 20 m. This is an indication that the weathered laterite extend down at a much longer depth and at the Northern corner of the study area (VES D3). This region has resistivity value ranging between 200 Ωm to 500 Ωm and it can be seen that the proceeding region has a low resistivity at the northern part of the study area with resistivity value ranging between 30 Ωm to 150 Ωm. This is attributed to presence of ground water.

Deductions from Vertical Geoelectric Section
Deductions from Profile A
The vertical section of profile A is as shown in Figure 7a while the corresponding geologic section is shown in Figure 7b. The map is contoured at the interval of 100 Ωm. This map can be divided into three layers structure, with each layer comprising of different lithologies.

The first layer has a relatively high resistivity value range of 18.6 Ωm – 349.3 Ωm which indicates absence of contaminant. The layer suggests a region of dry sandy soil (Table 3.2) of the first and second layer is an indication of dry sandy soil which is free from pollution. The second layer suggests weathered basement with resistivity value rage of 69.82 Ωm – 413.5 Ωm. the third layer has a resistivity value ranging from 802.65Ωm to 1748.7Ωm which is an indication of fresh basement.

Deductions from Profile B
The vertical section of profile B is as shown in Figure 8a while the corresponding geologic section is shown in Figure 8b. The map is contoured at the interval of 50 Ωm. this map can be divided into three layers structure, with each layer comprising of different lithologies.

The first layer resistivity value range of 0.6 Ωm – 42.2 Ωm are low which may be leachate deposited as a result of refuse dump. The low apparent resistivity end <80 Ωm could be attributed to contamination of the groundwater due to leachate invasion (Abdullahi *et al*, 2010). The second layer suggests weathered basement with resistivity value range of 7.35 Ωm – 1925.0 Ωm. 7.35 is observed only in VES Point B2. Every other VES points have resistivity values ranging from 145.4 to 1925.0 which suggest a rock type of gravel. The third layer has a resistivity value ranging from 112.2 Ωm – 873.3 Ωm which is an indication of fresh basement.

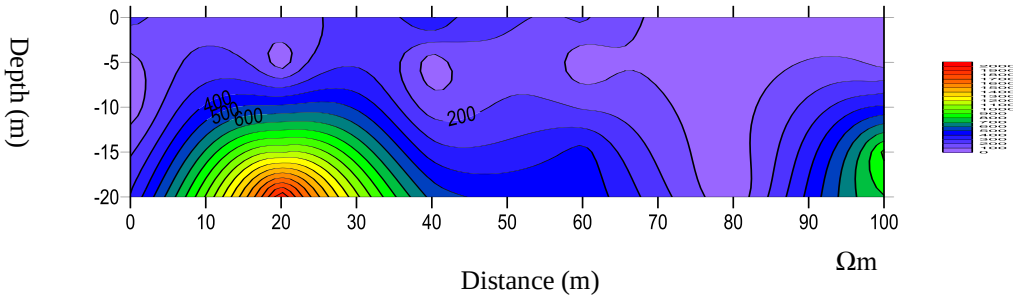

Figure 7a: Vertical Geoelectric Section on Profile A

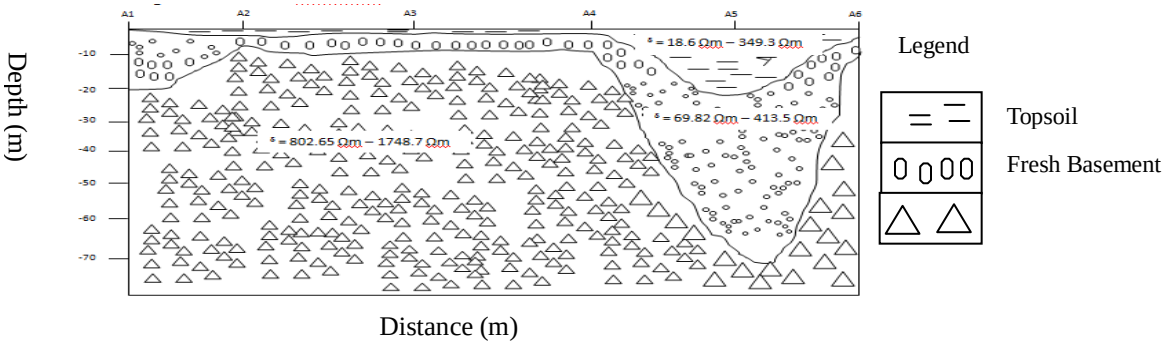

Figure 7b: Vertical Geoelectric (geologic) Section on Profile A

Deductions from Profile C

The vertical section of profile C is as shown in Figure 9a while the corresponding geologic section is shown in figure 9b. The map is contoured at the interval of 100 Ωm. this map can be divided into three layers structure, with each layer comprising of different lithologies.

The first layer has a resistivity value range of 0.9 Ωm – 248.8 Ωm which indicates presence of contaminant because 0.9 Ωm – 7.1 Ωm dominate the profile while 248.8 Ωm was noticed only at VES point C1 which is as a result of non-biodegradable and resistive waste material. The second layer suggests weathered basement with resistivity value rage of 27.2 Ωm – 2446.6 Ωm. Meanwhile, VES points C1 and C6 indicates basement at this layer with resistivity values of 2446.6 Ωm and 1619.0 Ωm respectively. The third layer has a resistivity value ranging from 112.0 Ωm to 23619.5Ωm which is an indication of fresh basement.

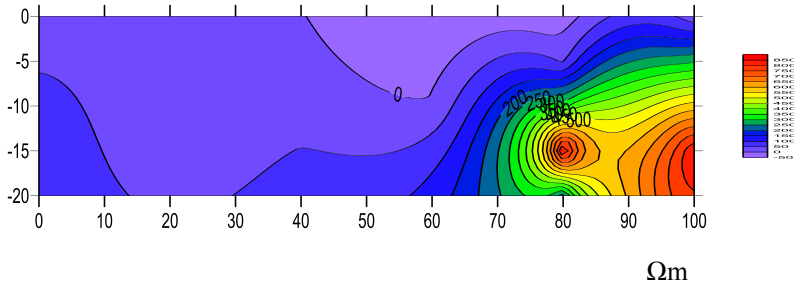

Figure 8a: Vertical Geoelectric Section on Profile B

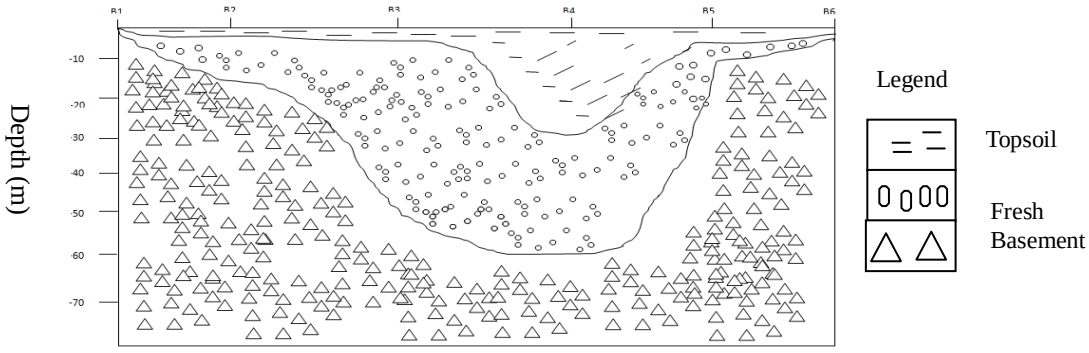

Figure 9a: Vertical Geoelectric Section on Profile C

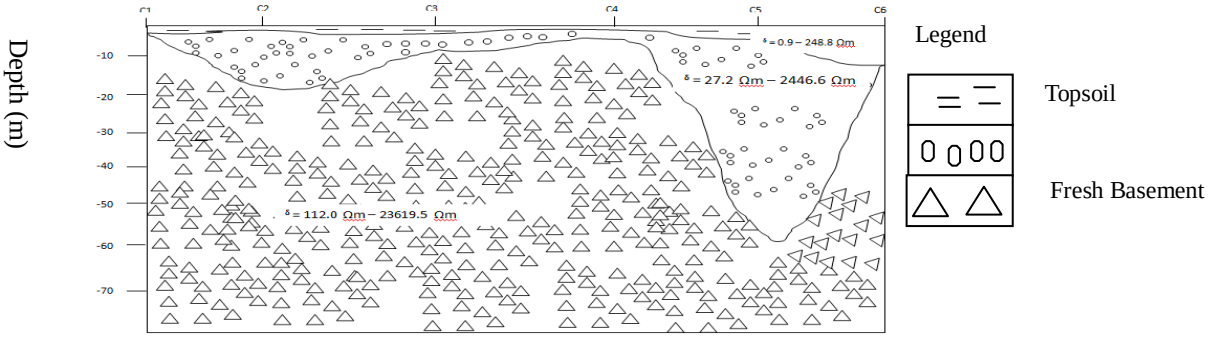

Figure 9b: Vertical Geoelectric (geologic) Section on Profile C

Deductions from Profile D

The vertical section of profile D is as shown in Figure 10a while the corresponding geologic section is shown in figure 10b. The map is contoured at the interval of 50 Ωm. this map can be divided into three layers structure, with each layer comprising of different lithologies.

The first layer has a relatively high resistivity value range of 1.2 Ωm – 85.6 Ωm which indicates presence of contaminant. The second layer suggests weathered basement with resistivity value range of 43.7 Ωm – 18693.8 Ωm. However, resistivity value 43.7 Ωm – 224.78 Ωm dominates the profile except VES point D4 which signifies fresh basement at this layer with resistivity value 18693.8 Ωm. The third layer has a resistivity value ranging from 414.7 Ωm to 31832.9 Ωm which is an indication of fresh basement.

Deductions from Profile E

The vertical section of profile E is as shown in Figure 11a while the corresponding geologic section is shown in figure 11b. The map is contoured at the interval of 2 Ωm. this map can be divided into three layers structure, with each layer comprising of different lithologies.

The first layer has a relatively high resistivity value range of 0.6 Ωm – 19.5 Ωm which indicates presence of contaminant. The second layer suggests weathered basement (Table 4.1) with resistivity value rage of 0.2 Ωm – 233.9 Ωm. This also indicates a further incursion of leachate to layer two. The third layer has a resistivity value ranging from 48.35 Ωm to 529.4 Ωm which is an indication of fresh basement.

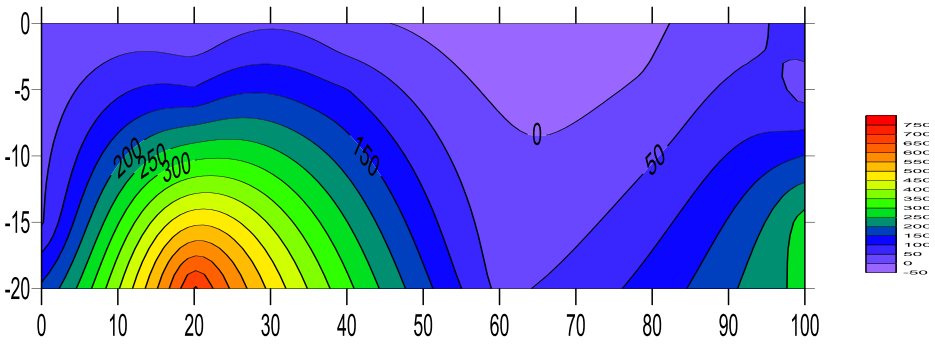

Figure 10a: Vertical Geoelectric Section on Profile D

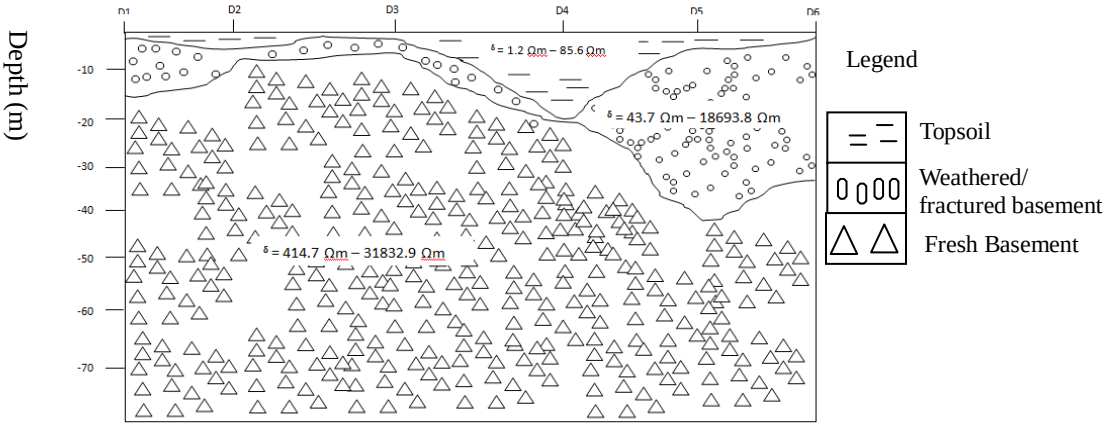

Figure 10b: Vertical Geoelectric (geologic) Section on Profile D

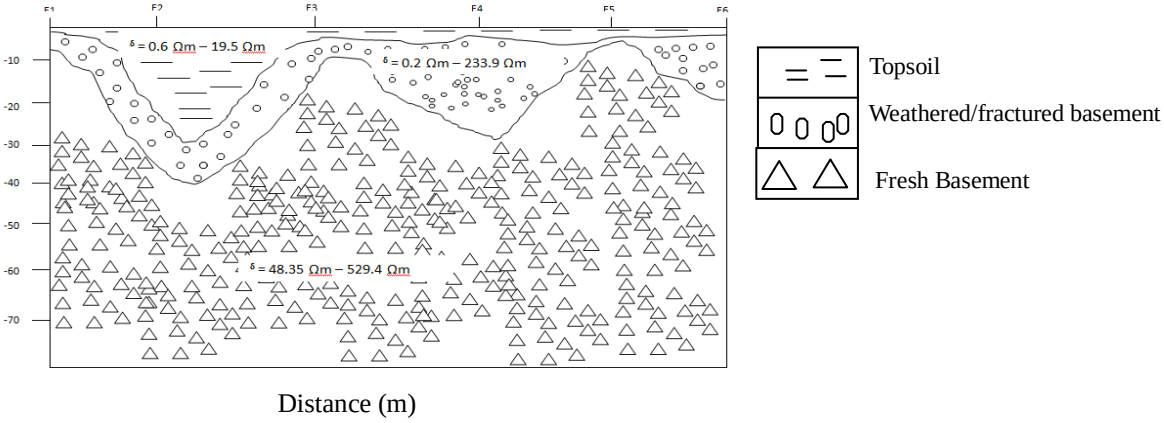

Figure 11a: Vertical Geoelectric Section on Profile E

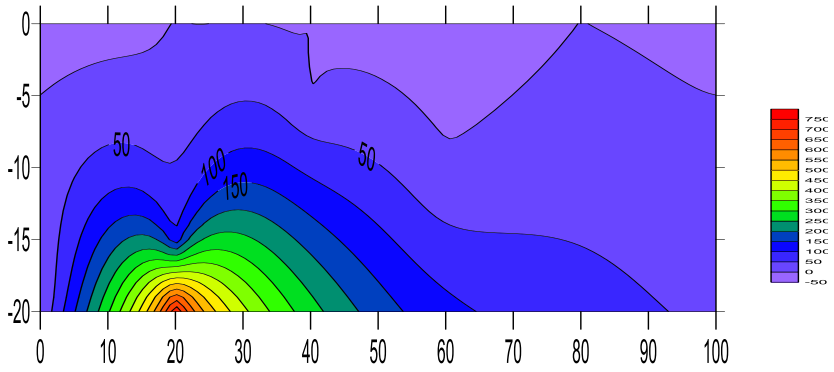

Figure 12a: Vertical Geoelectric Section on Profile F

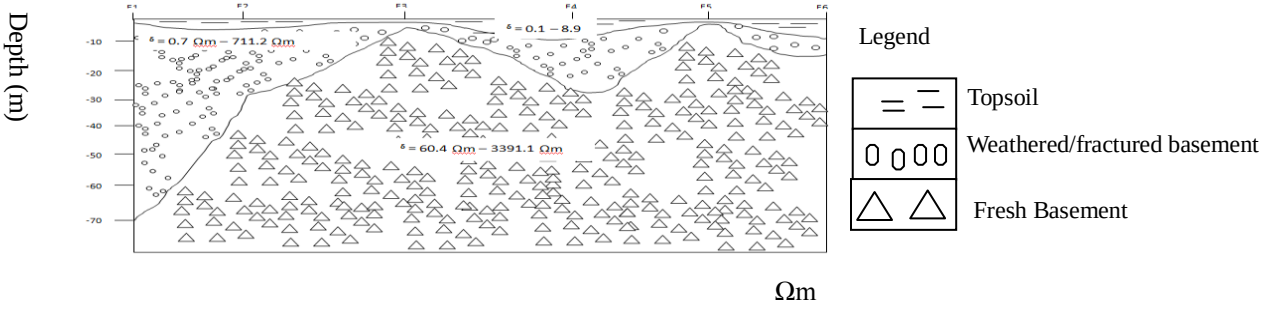

Figure 12b: Vertical Geoelectric Section on Profile F

Deductions from Profile F

The vertical section of profile F is as shown in Figure 12a while the corresponding geologic section is shown in figure 12b. The map is contoured at the interval of 50 Ωm. this map can be divided into three layers structure, with each layer comprising of different lithologies.

The first layer has a relatively high resistivity value range of 0.1 Ωm – 8.9 Ωm which indicates presence of contaminant. The second layer suggests weathered basement (Table 4.1) including traces of leachate with resistivity value rage of 0.7 Ωm – 711.2 Ωm. The third layer has a resistivity value ranging from 60.4 Ωm to 3391.1 Ωm which is an indication of fresh basement.

Lithology of Leacheration

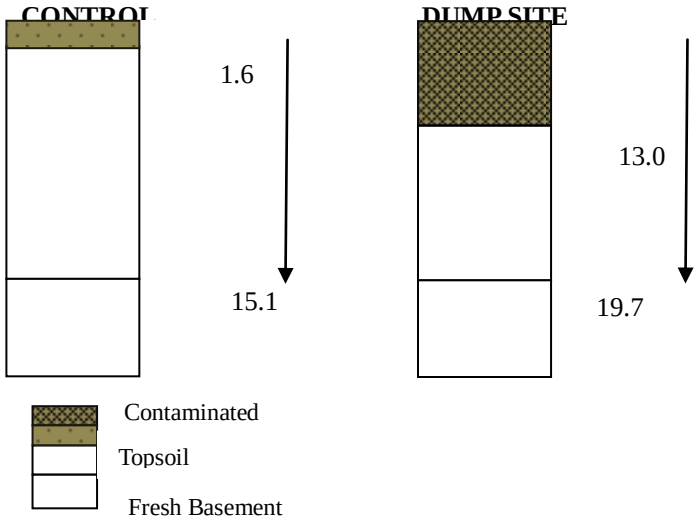

Figure 13: Correlation of Subsurface lithology and their average depth

Figure 13 5 shows the correlation of subsurface lithology and their average depth which was used to summarise the migration of leachate on the dump site. The dump and control sites are located in an area with the same geologic characteristics and the lithology at all layers are expected to be the same. However, due to continuous migration of leachate into the subsurface on the dump site, the layers on the dump sites are relatively conductive compared to the control site because of the presence of ions in the contaminants. Therefore, the iso-resistivity maps presented in Figures 3 through 6 above confirms that the resistivity values on the dump site are lower as compared to that of the control site. This disparity in resistivity value is observed up to the depth of 13 m. Figures 4.13a and 4.13b shows the iso-resistivity map at 13m for both dump and control sites respectively which indicates similarities in lithology signifying the end of contaminant percolation.

Aquifer Location

The results presented in the weathered/ fractured layer thickness map above indicates that VES points A5, B4, C5, D5, F1 and F4 have a promising aquifer potential. The fractured

Layer has a thickness of 20-46m and resistivity value ranging from 27.2-409.4 Ωm. According to Odusanya and Amadi (1990) reported by Abdullahi and Udensi (2008), the electrical resistivity of this layer, forms the water bearing zone, depends on the sand to clay ratio and degree of saturation. The zone with resistivity above 100 Ωm is characteristics of clayey sand and sand and it indicates good aquifer formation while the lower end (below 100 Ωm) typifies clay which lowers the aquifer potential.

CONCLUSION

Results from VES graph and vertical geo-electric section maps in previous chapters indicate the ingress of leachate into the subsurface up to the depth of about 13 m (Figure 7). The study area is mostly characterised by three (3) layered geologic sections which includes topsoil, weathered basement and Fresh basement. Based on the findings which are evident in the iso-resistivity contour maps presented (figure 3-6) , we suspect the subsurface at a depth of about 13 m to be contaminated by leachate migration. At the surface of the dump site, the resistivity value ranges from 20 Ωm to 40 Ωm as compared to that of the control site which ranges from 380 Ωm to 820 Ωm at the same depth. This indicates that the topsoil has been contaminated by leachate from the dump site. At 5 m depth, the resistivity value of the dump site ranges from 5 Ωm to 45 Ωm as against that of the control site at the same depth which is between 60 Ωm to 200 Ωm indicating migration of contaminants to that depth. The resistivity value for 10 m depths further indicates the presence of leachate as the dump site ranges from 20 Ωm to 60 Ωm and that of control site ranges from 260 Ωm to 580 Ωm. At 13 m depth, resistivity value at dump site ranges from 100 Ωm to 850 Ωm and that of the control site ranges from 200 Ωm to 850.This similarity in resistivity value at this depth influences the conclusion that the migration of leachate ends at 13 m. However, the aquifer is observed to be promising at the depth of 20 m. this suggests that the ground water is not contaminated. But if the migration continues at the current rate of 1.63m/year, the ground water will be contaminated in 12.3 years.

RECOMMENDATIONS

Towards the control of ground water vulnerability to pollution through landfills, there is need for adequate and proper planning, design and construction, and strategic management of waste disposal. Government at all levels should consider facing out the ordinary landfill system and provide modern sanitary landfills to ameliorate the incessant ground water contamination.

Detailed analysis of hydrogeology and ground water flow direction in proposed dump sites is required to safeguard the ground water system from pollution. Agencies such as Niger State Environmental Protection Agency (NISEPA) should engage in more research to monitor contaminant levels and plan mitigation strategies.

REFERENCES

Asurimen, Mike (2008). 2-D electrical resistivity investigation of solid waste dump site at Gonin-Gora, Kaduna State Nigeria. MSc thesis: Department of Physics, Ahmadu Bello University, Zaria, Nigeria

Abdullahi, N. K., and Udensi, E. E., (2008). Vertical Electrical Sounding Applied to Hydrogeologic and Engineering investigatios: A case study of Kaduna polytechnic staff quarters, Nigeria. Nigeria journal of Physics, 20(1) pp 175-189

Aderoju, O. M., Salman, S. K., Anjoye, S., Nwadike, B., Jantiku, J., Adebowale, R. K.,Fagbemiro, O. A., andAgu N. V. (2014). A Geo-Spatial Approach for Solid Waste Dumpsites for Sustainable Development in Minna, Niger State, Nigeria. IOSR Journal of Environmental Science, Toxicology and Food TechnologyVol. Vol. 8 (10), pp. 16-28.

Adeniyi, J. O. (1985). Geophysical Investigation of the Central Part of Niger State of Nigeria. Ph.D thesis, University of isconsin, Madison. USA.

Jatau, B.S. and Ajodo, R.O. (2006): Preliminary Geo-environmental evaluation of parts of Kaduna North metropolis, Kaduna, Nigeria. A paper presented at the Nigeria Association of Hydrogeologists (NAH) 18th Annual National Conference Asaba, pp. 1-2.

Manoj P. Wagh, Piyush K. Bhandari, SwapnilKurhade., (2014): Ground Water Contamination by Leachate. International Journal of Innovative Research in Science, Engineering and Technology (IJIRSET) Vol 3(4), pp. 148-152.

Mohammed, I. N, Aboh, H. O. &Emenike, E. A.. (2008): Hydrogeophysical investigation for groundwaterPotential in Central Minna, Nigeria. Science World Journal Vol 3 (NO4), pp. 49-54.

Udensi, E.E., Ogunbanjo, M.I., Nwosu, J.E., Jonah S.A., Kolo, M.T., Onuduku, U.S., Grown, I.E., Daniyan, M.A., Adeniyi, J.O., & Okosun, F.A. (2005). Hydrogeological and Geophysical Surveys for groundwater at designated premises of the main Campus of the Federal University of Technology, Minna; Zuma Journals of Pure and Applied Science (ZJ PAS). 7 (1), pp. 52-58.